

A proposal for optical high-accuracy atomic references using thin cell spectroscopy

N. Beverini

Dipartimento di Fisica dell'Università di Pisa
CNISM, unità di Pisa
Pisa, Italy
beverini@df.unipi.it

A. Ch. Izmailov

Institute of Physics of the
Azerbaijan National Academy of Sciences
Baku, Azerbaijan
azad57@mail.ru

Abstract—We analyze here a scheme for sub-Doppler spectroscopy of an atomic transition connecting a ground state level with a metastable one, which exploits the asymmetric absorption properties of a single pump beam, propagating along the axis of a shallow cell. If the metastable lifetime is large enough, the interaction between the atom and the resonant radiation is interrupted mainly by the collisions against the walls, and only atoms with a small longitudinal velocity component interact with radiation long enough to undergo a transition, producing sub-Doppler selective excitation. Possible application to optical atomic reference standard is discussed, based on alkali-earth atom forbidden transitions.

I. INTRODUCTION

A cell standard based on the forbidden transitions of alkali atoms would be of great relevance, because these transitions are the most promising as references for the optical atomic clocks now under development. The availability of a cell reference at the same frequencies opens new, very interesting perspectives. First of all, this can be a first step toward the stabilization of the lasers that will be locked to ultracold atoms. But the most relevant point could be the availability of atomic standards, potentially with an accuracy at 10^{-12} level, operating in cell, with very small sizes, mass and electrical consumption, so that they will be easily transportable and suitable also for satellite operation.

In a recent paper we proposed a new scheme of sub-Doppler optical spectroscopy of forbidden transitions from ground state to a metastable level of an atomic vapor contained in a thin cell [1]. In the following, we will first briefly recall the theoretical basis (ch. II), and then we will discuss the foreseeable performance of a cell frequency reference based on this method (ch.III), giving also some suggestions about the possible realization of a similar apparatus.

II. THEORETICAL BASIS

The proposed sub-Doppler spectroscopy scheme applies to transition between the ground state and a long-lived metastable level, like is the case in alkali-earth atoms of the

lowest energy triplet state 3P_1 or the the lowest energy 1D_2 state (connected to the ground state respectively by a spin-forbidden intercombination line and an electric quadrupole line).

Let's consider a transparent cell of radius R and inner length $L \ll R$ containing an atomic vapour at a density N low enough, in order to have an interatomic collisional mean free path $l_c \gg L$. If we irradiate the cell uniformly with a monochromatic radiation in resonance with a first-order forbidden transition connecting the ground state to a metastable level, the probability of an atom initially in the ground state being excited into the metastable level is proportional, at low saturation, to $g^2 T^2$, being g Rabi's frequency and T the coherent atom-radiation interaction time. Thus, absorption probability acquires an asymmetric dependence on the longitudinal component of the atomic velocity, and sub-Doppler velocity selective excitation is produced. The absorption probability will be much higher for atoms whose velocity component along the propagation axis of the excitation beam is close to zero, for which $T \approx R/u$, where u is the thermal most probable atomic speed.

This selective excitation can be eventually detected by using as a probe a second laser beam, resonant with a high-intensity transition starting from the metastable state.

A calculation of the effectiveness and the shape of this velocity selection, valid also in condition of no negligible saturation, has been performed in [1] in the formalism of density matrix equations for a two-level system, taking into account Rabi's coherent oscillations. In that paper we have shown that an annular pumping geometry (Fig. 1) can produce a more effective velocity selection. In this scheme a pumping beam, resonant with the transition, irradiates orthogonally an annular region with outer radius R and with a black central region of radius r_0 . In order to simplify the calculation, it was assumed the hypothesis of a uniform radiation power density over the irradiated volume. The atomic population density n in the metastable level is then monitored in a small region of radius r_1 , around the axis of the pumping beam. We analysed in detail the spin-forbidden transition from ground state to 3P_1

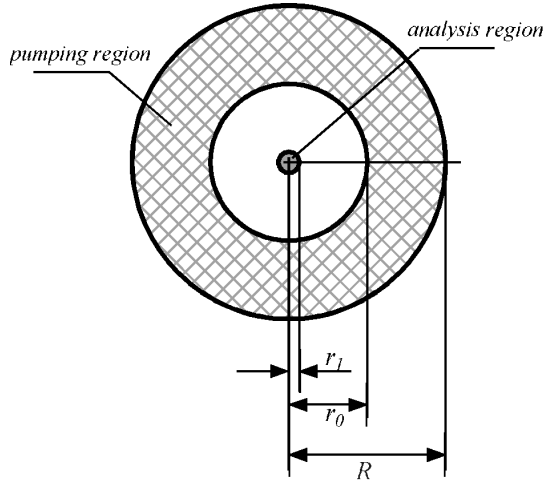


Figure 1. Irradiation of the thin gas cell (in the axial direction) by a monochromatic laser beam, having the ring-shaped cross-section with the external radius R and inner radius r_0 . The excited state population is probed by a second laser beam, in the central region of radius r_1 .

metastable level in Ca at 657 nm. Fig. 2 presents the fractional population n/N as a function of the laser frequency detuning δ from the centre of the transition $^1S_0 \rightarrow ^3P_1$ for $R=2.5$ cm, $L=10$ μm , $r_0=1.5$ cm and different values of the Rabi frequency g . We can see that, for low intensities of the laser radiation ($g \cdot (R/u) \approx 1$), the full width at the half maximum (FWHM) Δ is smaller by a factor $2.6 \cdot 10^{-4}$, close to $L/(2R)$, with respect to the characteristic Doppler broadening of the atomic gas in the cell $D=(2\pi/\lambda) \cdot u$, that is a reduction of a factor $6.4 \cdot 10^3$ with respect to the Doppler thermal FWHM given by $2\sqrt{\ln 2} D$.

Moreover, it should be noted the sharpness of the resonance curve. This sharpness can be effectively quantified

by the parameter $\eta = \frac{\Delta^2}{8n(0)} \left| \frac{\partial^2 n(\delta)}{\partial^2 \delta^2} \right|_{\delta=0}$ that is the normalized

value of the second derivative of the curve at the peak. The normalization has been done in order to obtain $\eta = 1$ for a Lorentzian shape. We found values ranging between 2.5 and 4.2 in all the cases where $g R/u \leq 3$ and $r_0/R \geq 0.4$, which must be compared with the value $\ln(2) \approx 0.693$ for a Gaussian shape.

Larger value of pump laser intensity produces a larger number of metastable atoms, at the price of a less effective velocity selection. Also the pumping geometry affects both the amplitude and the width of the resonance curve. The effect of changing the relative dimension of the inner radius r_0 of the irradiation annular region at a fixed value of the outer radius R is shown in Fig. 3, where the amplitude of signal A and the FWHM Δ on the axis are plotted as functions of the ratio r_0/R . As expected, by reducing the dimension of the central hole both the population density on the metastable level and the residual Doppler width increase. The sharp increasing of the resonance width for $r_0/R > 0.95$ in Fig.3b is due to the large time-of-flight broadening of the spectral line in these conditions. The best operative condition can be found by optimizing the ratio A/Δ . As shown in Fig. 4, for low intensity the best conditions are obtained for quite small dimension of

the radius of black central region, while for a higher saturation value it is more convenient keep a value of $r_0/R \approx 0.6$.

A similar theoretical scheme can be applied also to spin-forbidden transition from ground state to 3P_1 metastable level or to electric quadrupole transition from ground state to 1D_2 metastable level of other alkali-earth atoms. In Table I we summarised the most important parameter for these transitions. In order to obtain an efficient velocity selection it is obviously required that the decay length l_d of the transition (calculated as the path covered by an atom moving at the rms thermal velocity u during one decay lifetime) should be longer than the radiation beam diameter $2R$. Also the collisional free mean path l_c of the atoms must be substantially larger than $2R$; for this reason we have considered in all the case a working temperature equivalent to an atomic saturated vapour pressure of 10^{12} cm^{-3} so that $l_c \gg 1$ m.

It should be noted that Ca and Sr quadrupole transitions are not a transition closed, because the 1D_2 level can decay also on the less energetic 3P_1 and 3P_2 levels. At opposite, 1D_2 level in Ba is the metastable level with the lowest energy.

III. APPLICATION TO ATOMIC FREQUENCY STANDARDS

A. Detection Schemes

It should be possible to detect the sub-Doppler resonances simply monitoring the fluorescence due to the radiative decay of the metastable atoms in the central black region of the annular laser beam. However, the fluorescence intensity will be quite low, and signal-to noise ratio will be quite poor, also for the unavoidable background due to the light scattered from the pumping beam.

More efficient schemes, valid also for transitions with very

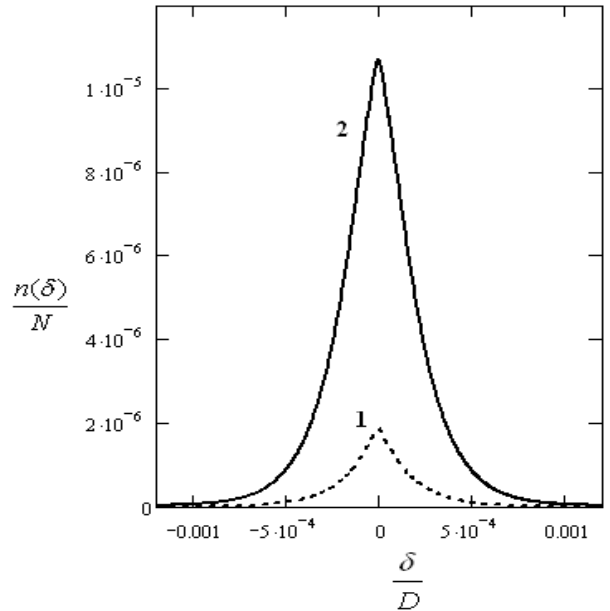


Figure 2. Population density n of the metastable level (in units of the atomic density N) versus the frequency detuning δ (in units of the Doppler broadening D). when $R=2.5$ cm, $L=10$ μm , $r_0=1.5$ cm, $[R/L=2500, r_0/R=0.6]$, $g \cdot (R/u)=1$ (curve 1) and $g \cdot (R/u)=3$ (curve 2).

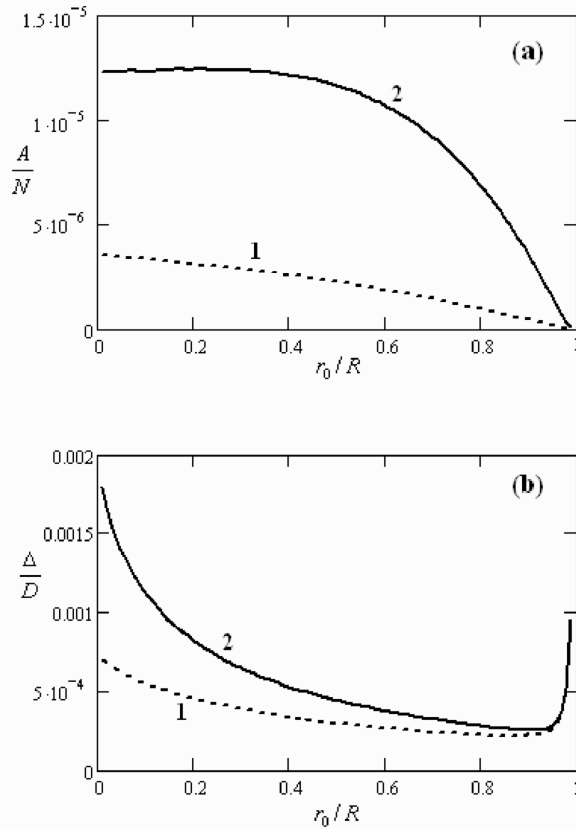


Figure 3. Amplitude A (a) and width Δ (b) of the population spectral distribution $n(\delta)$ as a function of the radius ratio r_0/R , when $R=2.5$ cm, $L=10$ μm [$R/L=2500$], $g \cdot (R/u)=1$ (curve 1) and $g \cdot (R/u)=3$ (curve 2).

long metastable level lifetime, are possible, by using a second probe laser, which is resonant with a transition leaving from the metastable level. It is convenient to direct this additional radiation coaxially to the pumping beam inside the central dark hole (the region with a radius r_1 in Fig.1). In this way, due to the spatial separation of these light fields in a gas cell, the probe radiation will not affect on the optical velocity selection of metastable atoms induced by pumping beam. In this case the number of collected fluorescence photons is simply limited by the diffusion rate of metastable atoms inside the detection volume ($\approx u/r_1$). Moreover, it is possible in this scheme to use a phase sensitive detection technique by frequency modulating the pumping beam, allowing the discrimination of the fluorescence photons from the scattered ones. A large suppression of the background radiation can be obtained, if a probe transition is chosen that produces fluorescence mostly on a different spectral region from absorption. Alternatively, the use as probe of a close transition leaving from the metastable level can greatly increase the number of fluorescence photons produced by a single metastable atom, with a consequent reduction of the shot noise.

B. Frequency Standards Accuracy

The accuracy performance of a cell optical frequency standard based on this scheme can be quite interesting. It

cannot obviously achieve the precision of cold atom or of atomic beam spectroscopy, but it may favorably compete with other more cumbersome techniques of sub-Doppler spectroscopy.

Let us analyze the different sources of inaccuracy of the resonance line. The fractional second-order Doppler effect can be computed approximately as $\frac{1}{2} u^2/c^2$. Its value is $1.6 \cdot 10^{-12}$ for *Ca*, $0.7 \cdot 10^{-12}$ for *Sr*, $0.4 \cdot 10^{-12}$ for *Ba*, by considering the most probable velocity at the temperature equivalent to a vapor pressure density of 10^{12} cm^{-3} . If we assume conservatively an uncertainty of the order of 10% on these values, we find that that second-order Doppler effect does not affect the accuracy, almost at a level of 10^{-13} .

Also the sensitivity to external magnetic field is not a problem at a level of 10^{-13} , if the pump polarization is chosen in order to excite $m_j=0 \leftrightarrow m_j=0$ component

Light shift can be an important factor. Roughly, light shift can be estimated of the same order of magnitude of the transition Rabi frequency. A target for accuracy of 10^{-12} means 150 – 350 Hz, following the different transition frequencies. Assuming a pump intensity stabilized at 1% level, we will have a constrain on Rabi frequency $g \leq 2\pi \cdot 1.5 \cdot 10^4$ rad/s $\approx 9 \cdot 10^4$ rad/s, which means for the considered geometry that the parameter $g(R-r_0)/u$ should be lower than 4.5.

In principle, possible misalignments between the laser beam direction and the cell axis should affect the resonance profile. However, provided that the axial symmetry of the pumping beam is respected, this will broaden the sub-Doppler profile, but will not shift its centre. On the contrary, the effect due to the curvature of the wave front should produce a line asymmetry, but it is not too difficult to obtain good planarity in a Gaussian beam with a waist radius of 2.5 cm.

Collisional effect can be kept under control, provided that the atomic mean free path is long enough (at a density of 10^{12} cm^{-3} it is longer than 1 m). It requires to keep a high-quality vacuum in the cell, which is not an easy job.

C. A Calcium Standard

The case of the metastable $(4s4p)^3P_1$ calcium level and of the corresponding spin-forbidden transition at 657 nm has

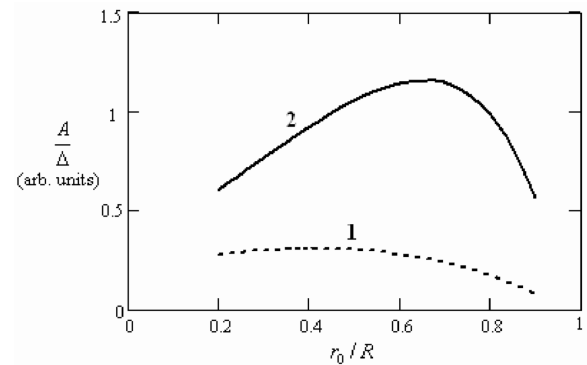


Figure 4. Ratio A/Δ between the amplitude and the width of the population spectral distribution $n(\delta)$ as a function of the radius ratio r_0/R , when $R=2.5$ cm, $L=10$ μm [$R/L=2500$], $g \cdot (R/u)=1$ (curve 1) and $g \cdot (R/u)=3$ (curve 2).

been already analyzed in [1]. An useful transition for the probing can be the intercombination line $(4s4p)^3P_1 \rightarrow (4s5s)^1S_0$ at 552.1 nm, which decays emitting a photon at 1.034 μm and at 422.6 nm. The photon at 422.6 nm can be easily discriminate from pump and probe radiation, allowing a background free detection. In the condition of curve 2 in Fig. 2 ($L=10 \mu\text{m}$, $R=2.5 \text{ cm}$, $g\text{-}R/u=3$, $r_0=1.5 \text{ cm}$), with an atomic density $N=10^{12} \text{ cm}^{-3}$, we have $n(0) \approx 1.05 \cdot 10^7 \text{ cm}^{-3}$ and a residual Doppler FWHM $\Delta \approx 300 \text{ kHz}$. Thus, we estimate the flux of fluorescence photons available on the photodetector as:

$$n_{\text{fl}} = \varepsilon \frac{\sigma}{4\pi} \frac{n(0)V}{r_1/u} = \frac{\varepsilon\sigma}{4} u n(0) r_1 L \approx 3.2 \cdot 10^6 \text{ photons/s},$$

where V is the probed cylindrical volume, with radius $r_1 = 2.5 \text{ mm}$ and height L , and we consider a quantum efficiency ε of the detector of 90%, and a collection angle $\sigma = 1/10$ sterad. The shot noise limit at 1 s is then $\Delta(\eta \cdot n_{\text{fl}})^{-1/2} \approx 100 \text{ Hz}$, that is about $2.2 \cdot 10^{-13}$.

A more convenient choice may be the use as probe of the closed transition $(4s4p)^3P_1 \rightarrow (4p2)^3P_0^o$ at 430 nm, which do not destroy the metastable level population, and can recycle a single metastable atom more than 1000 times during its crossing the probe beam, increasing the signal level at the price of the presence of scattering background. Moreover, the wavelength of 430 nm can be easily obtained from diode laser.

For calcium atom it is possible also to consider the quadrupole transition to the $(3d4s)^1D_2$ metastable level at 457 nm. Also in this case a cyclic transition is available as probe (the $(3d4s)^1D_2 \rightarrow (3d4p)^1D_2^o$ transition at 714 nm). An interesting option come from the fact that 1D_2 level decays preferably through the triplet 3P levels. This gives the opportunity to detect the metastable population, without using any probe beam, by simply observing the fluorescence, free

from scattered background, of the 3P_1 level at 657 nm.

D. Other Alkali-Earth Atomic References

In the case of *Sr*, the short lifetime of the 3P_1 level limits the application of the technique to the 689.5 nm intercombination line. It is more interesting the case of the E2 transition to the $(4d5s)^1D_2$ level at 496.3 nm. In this case it can be used as a probe the 717 nm $4d5s^1D_2 \rightarrow 5s6p^1P_1^o$ transition, which then decays preferably directly on the ground state emitting an UV 293 nm photon. Also it is available a suitable close transition $(4d5s^1D_2 \rightarrow 4d5p^1D_2^o)$ at 730.9 nm). The option of directly observe the 1D_2 level decays through the 3P_1 level fluorescence at 689.5 nm can be more effective than in the similar already examined *Ca* case, because the much shorter lifetime of 3P_1 level.

With *Ba* the E2 transition at 877.4 nm is very promising. Lifetime of this level has been measured of about 120 ms [2]. The higher vapour density of *Ba* gives the opportunity to operate at lower temperature (310°C with respect to the 445°C necessary for *Ca*), simplifying the technical problems. A suitable probe cyclic transition (the $5d6s^1D_2 \rightarrow 5d6p^1D_2^o$ at 856.0 nm) is available. Both these wavelengths can be easily obtained from commercial diode laser. Due to the heavy atomic weight of *Ba*, the Doppler width is smaller by a factor 1.85, giving the possibility to achieve, in a scheme similar to that described before for *Ca*, a better accuracy and stability.

E. Highly forbidden transitions

A reference cell with thin depth can be also a useful tool in order to provide a first reference for the laser to be used in the new generation of atomic clocks, based on the highly forbidden transitions $^1S_0 \rightarrow ^3P_0$. Lattice-based clocks using the $^1S_0 \rightarrow ^3P_0$ transitions in the odd isotopes of alkaline earth-like atoms were first proposed and demonstrated in *Sr* by Katori et al [3], while at NIST a new method has been developed that uses a small magnetic field ($\sim 1 \text{ mT}$ or 10 G) to achieve in even isotopes the requisite level mixing but with much smaller magnetic field sensitivity for the clock transition [4]. Different groups in the world are at present working on developing such types of atomic clocks both on *Sr* and *Yb* atoms [5,6,7,8]. The natural width of 3P_0 level in fermionic *Sr* and *Yb* is of the order of 10 mHz, while in the case of bosonic isotopes it is a function of the applied magnetic field, and can achieve 1 Hz in a field of the order of 1 mT (10 gauss). The absorption resonance can be monitored by using as a probe the $^3P_0 \rightarrow ^3S_1$ transition (at 679 nm for *Sr* and at 707 nm for *Yb*) and detecting (branching ratio efficiency 5/9) the fluorescence of the $^3S_1 \rightarrow ^3P_2$ transition at 649 nm and 770 nm, respectively.

IV. HOW TO BUILD THE THIN RESONANCE CELLS

Building shallow cells for containing the alkaline earths can be a hard task, requiring sophisticated techniques. While with alkali atoms, in particular Rb and Cs, it is possible to operate near room temperature or only slightly above, thus allowing the use of Pyrex or quartz cells, alkaline-earth elements reach a suitable vapour density only at relatively high temperatures, between 400 °C and 500 °C. At these temperatures the alkaline-earth atoms are chemically strongly reactive, restricting the choice of possible transparent

TABLE I. THE MOST IMPORTANT PHYSICAL PARAMETERS FOR ALKALI-EARTH FORBIDDEN TRANSITIONS LEAVING FROM 1S_0 GROUND STATE (λ : TRANSITION WAVELENGTH; A_{ik} : TRANSITION PROBABILITY; τ : METASTABLE STATE LIFETIME; T : TEMPERATURE CORRESPONDING TO A VAPOR PRESSURE OF 10^{12} cm^{-3} ; u : MORE PROBABLE THERMAL ATOMIC VELOCITY AT TEMPERATURE T ; l_d : MEAN DECAY LENGTH):

Metastable Level	λ nm	A_{ik} s^{-1}	τ s	T K	u m/s	l_d cm
Mg – 3P_1	457	200	$5.0 \cdot 10^{-3}$	591	640	320
Ca – 3P_1	657	2900	$3.4 \cdot 10^{-4}$	718	546	19
Ca – 1D_2	457	54,4	$4.5 \cdot 10^{-3}$	718	546	250
Sr – 3P_1	689	47000	$2,1 \cdot 10^{-5}$	668	355	0.75
Sr – 1D_2	496	45	$3,0 \cdot 10^{-4}$	668	355	11
Ba – 3P_1	791	$3 \cdot 10^5$	$3,4 \cdot 10^{-6}$	582	265	0.089
Ba – 1D_2	877	8	0,12	582	265	330
Yb – 3P_1	555	$11 \cdot 10^5$	$9,1 \cdot 10^{-7}$	688	256	0.023
Yb – 1D_2	431	?	?	688	256	$\gg 100$

materials. Actually, above 300 °C they react even with quartz, which rapidly loses its transparency. Sapphire is the most suitable material, displaying also an ideal thermal conductivity, but its hardness gives origin to non-trivial technical problems for its treatment. Our suggestion is to realize the cell by carving through an ultrasound digitally controlled milling-machine a cylindrical cavity on an optically flat sapphire slab [9]. By this method it is possible to obtain cavities with a diameter up to 10 cm or more and a depth between a ten of μm and 1 mm. High quality surface flatness is not required, and for the roughness it will be sufficient to optically polish the worked surface by lapping. Ultrasonic technology give also the possibility to carve in the sapphire slab a linear groove, may be 1 mm deep and a few cm long, joining the cell cavity with a second small cavity, depth approximately 2 - 3 mm, to be used as a reservoir. The worked sapphire slab will be cleaned in a white chamber, and a grain of chemically pure metal will be inserted into the reservoir. The cell will be closed in a facility for manipulation under high vacuum by optical contact against a second sapphire slab. If necessary, it may be possible also to braze under vacuum the two slabs together.

V. CONCLUSIONS

We have presented here a new possible scheme for building an optical atomic frequency standard in cell, by exploiting the velocity selective asymmetric absorption of the resonant radiation in a thin cell. This scheme appears

promising for the realization of small dimension, small weight, and small power requirement optical frequency standard with satisfactory performances.

REFERENCES

- [1] N. Beverini, and A.Ch. Izmailov, "Sub-Doppler spectroscopy of atoms excited in the regime of Rabi oscillations in a thin gas cell," *Opt. Commun.* (in press), doi:10.1016/j.optcom.2009.03.018 .
- [2] I. I. Klimovskil, P. V. Minaev, and A. V. Morozov, "Measurement of the probabilities of forbidden radiative transitions in the barium atom," *Opt. Spectrosc. (USSR)* vol. 50, 1981, pp.464-467 [*Opt. Spektrosk.* vol. 50, pp. 847-852, 1981].
- [3] M. Takamoto, F.-L. Hong, R. Higashi, and H. Katori, *Nature (London)* "An optical lattice clock," vol. 435, pp. 321-324, May 2005.
- [4] A.V. Taichenachev, et al., "Magnetic field-induced spectroscopy of forbidden transitions with application to lattice-based optical clocks," *Phys. Rev. Lett.* vol. 96, 2006, 083002.
- [5] M. Yasuda, F.-L. Hong, T. Kohno, H. Inaba and K. Hosaka, "Present status of the development of an Yb optical lattice clock at NMIJ/AIST," *Proc. SPIE*, vol. 6673, 2007, p. 66730D.
- [6] Campbell G.K., et al. "The absolute frequency of the ^{87}Sr optical clock transition," *Metrologia* vol. 45, 2008 pp. 539–548.
- [7] J. Courtillot, et al., "Accurate spectroscopy of Sr atoms," *Eur. Phys. J.* vol. 33, 2005, pp.161-171.
- [8] N. Poli et al., "Cooling and trapping of ultracold strontium isotopic mixtures," *Phys. Rev. A* vol. 71, 2005, 061403.
- [9] A. Bertolini, et al.: "5-axis CNC ultrasonic cutting machine: design and preliminary test," LIGO Technical Note T020198R-00-R, 2002, <http://www.ligo.caltech.edu/docs/T/T020198-00>.